

Molecular Docking Study Based on Pharmacophore Modeling for Novel PhosphodiesteraseIV Inhibitors

Gülşah Çıfci,^[a] Viktorya Aviyente,^{*[a]} and E. Demet Akten^{*[b]}

Abstract: In this study, pharmacophore modelling was carried out for novel PhosphodiesteraseIV (PDEIV) inhibitors. A pharmacophore-based virtual screening, which resulted in 1959 hit compounds was performed with six chemical databases. The pharmacophore screening was proven to be successful in discriminating active and inactive inhibitors using a set of compounds with known activity obtained from ChEMBL database. Furthermore, the Lipinski's rule of five was applied for physicochemical filtering of the hit molecules and this yielded 1840 compounds. Three docking software tools, AutoDock 4.0, AutoDock Vina, and Gold v5.1 were used for the docking process. All 1840 compounds and the known selective inhibitor, rolipram, were docked into the active site of the target protein. A total of 234 compounds with all three scoring values higher than those of rolipram were determined with the three docking

tools. The interaction maps of 14 potent inhibitors complexed with PDEIV B and D isoforms have been analyzed and seven key residues (Asn 395, Gln 443, Tyr 233, Ile 410, Phe 446, Asp 392, Thr 407) were found to interact with more than 80% of the potent inhibitors. For each one of the 234 hit compounds, using the bound conformation with the highest AutoDock score, the interacting residues were determined. 117 out of 234 compounds are found to interact with at least five of the seven key residues and these were selected for further evaluation. The conformation with the highest AutoDock score for each 117 compounds were rescored using the DSX scoring function. This yielded a total of 101 compounds with better score values than the natural ligand rolipram. For ADME/TOX calculations, the FAF-Drugs2 server was used and 32 out of 101 compounds were found to be non-toxic.

Keywords: Molecular docking · Pharmacophore modeling · PhosphodiesteraseIV inhibitors

1 Introduction

Cyclic adenosine monophosphate (cAMP) and cyclic guanosine monophosphate (cGMP) are intracellular second messengers mediating the response of cells to a wide variety of hormones and neurotransmitters in signal transduction pathways.^[1-3] The families of cyclic nucleotide phosphodiesterase (PDE) enzymes are responsible for the degradation of cAMP or cGMP to 5'-AMP or 5'-GMP.^[4-6] The concentration level of cAMP or cGMP in vivo is important for many pharmacological processes such as pro-inflammatory mediator production and action, ion channel function, muscle contraction, learning, differentiation, apoptosis, lipogenesis, glycogenolysis and gluconeogenesis.^[1-3]


Up to now, 11 families of 21 human PDE genes were characterized by different substrate specificity (cAMP or cGMP), inhibition, substrate requirements, gene sequence and tissue distribution.^[1,2,4,7-11] One of these families belongs to PDEIV, a cAMP specific enzyme. The PDEIV isoform is a suitable drug target for a range of inflammatory and immune disorders like asthma and chronic obstructive pulmonary disease (COPD) and is also used as a therapeutic agent for rheumatoid arthritis, multiple sclerosis, type II diabetes, septic shock, atopic dermatitis, and other autoimmune diseases.^[12-17] There are about 20 potent inhibitors like rolipram, cilomilast, roflumilast (Scheme 1).^[18]

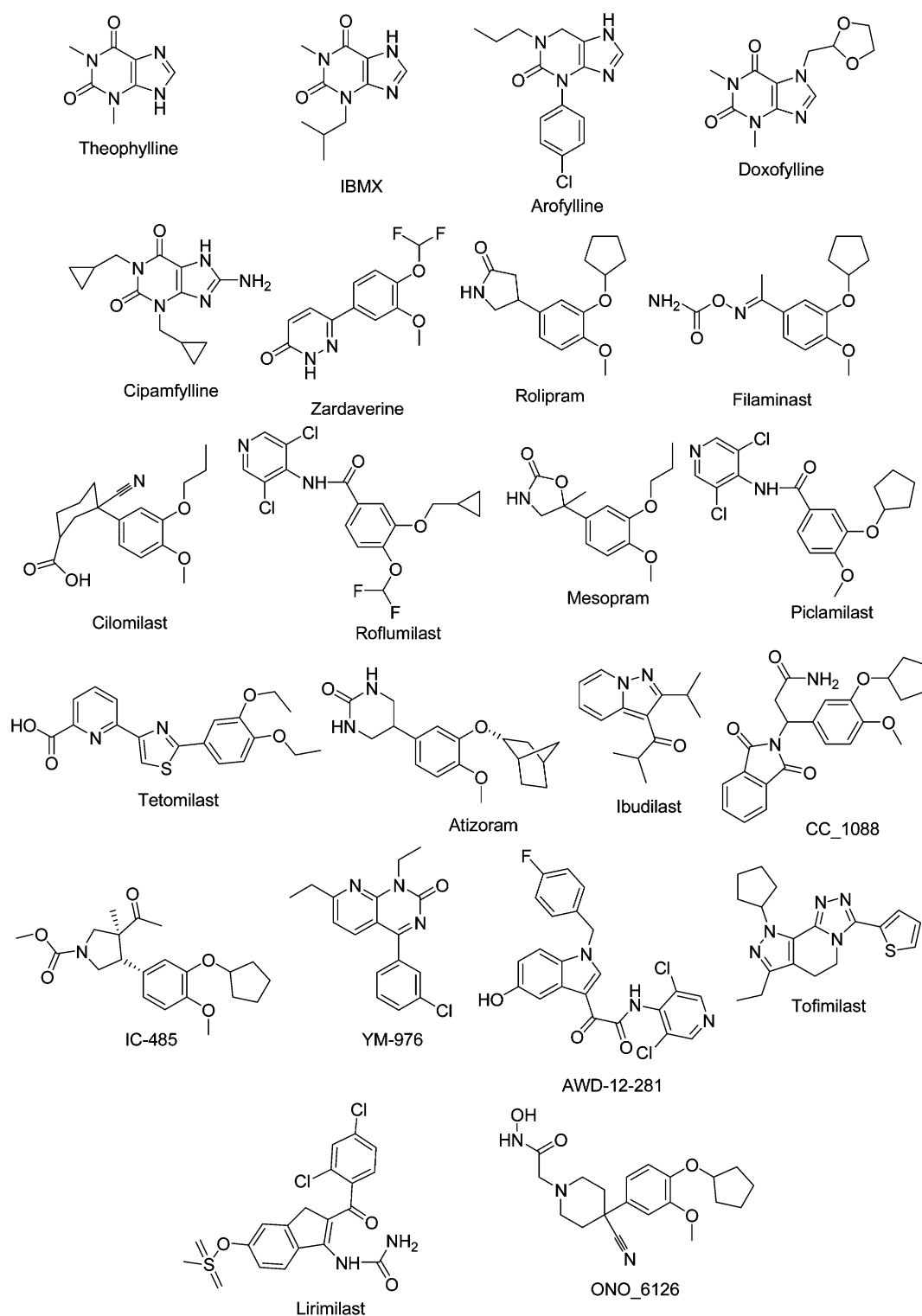
Rolipram is one of the earliest and most extensively studied PDEIV inhibitors. However it is known to be the cause of common side effects, such as nausea, headache and diarrhea.^[19-21] The potentially important clinical benefits of PDEIV inhibition, coupled with the limitations of current PDEIV inhibitors, highlight the need for novel PDEIV inhibitor chemotypes.^[22] Furthermore, mutations in the enzyme deactivate the enzyme,^[23] thus it is quite important to design new potent ligands for PDEIV.

The aim of this study is to suggest novel potent inhibitor structures for PDEIV with limited side-effects. For this purpose, structure-based pharmacophore models for PDEIV inhibitors were prepared and a library of compounds that fit

[a] G. Çıfci, V. Aviyente
Department of Chemistry, Boğaziçi University
34342 Bebek, Istanbul
*e-mail: aviye@boun.edu.tr

[b] E. D. Akten
Department of Information Technologies, Kadir Has University
34083, Cibali, Istanbul
*e-mail: demet.akten@gmail.com

 Supporting Information for this article is available on the WWW under <http://dx.doi.org/10.1002/minf.201100141>



Scheme 1. Potent inhibitors for PDEIV.^[18]

most the pharmacophore model is created. For virtual screening experiments, the docking process was carried out with three docking software tools, Autodock 4.0^[24] AutoDock Vina^[25] and Gold v5.1.^[26] The known active inhibitor,

rolipram, was also docked and its score value was set as the lower limit. The compounds that had score values higher than the lower limit in all three docking experiments were selected. Based on the MOE interaction maps, seven

residues (Asn 395, Gln 443, Tyr 233, Ile 410, Phe 446, Asp 392, Thr 407) interacting with more than 80% of the known potent PDEIV inhibitors as displayed in Scheme 1, are taken into account. Then, for each selected compound's most favorable binding pose, all the interacting residues are monitored and compared with the residues interacting with the potent inhibitors. The ligands that have interactions with at least five of the seven key residues are reselected and their highest-score conformations obtained from AutoDock are rescored using the DSX^[27] scoring function. This yielded a total of 101 compounds with DSX score values higher than that of rolipram. Finally, 101 compounds were filtered based on ADME/TOX calculation on the FAF-Drugs2 server^[28] and 32 compounds were found to satisfy the ADME properties and to be non-toxic.

2 Methodology

2.1 Pharmacophore Model and Database Generation

In this study, the pharmacophore models were generated with the software LigandScout^[29] with its default parameters. LigandScout yielded a total of eight pharmacophore models for four different PDEIV crystal structures taken from the Protein Data Bank (PDB codes: 1RO6, 1Y2J, 1XM4 and 2FM0). Then, pharmacophore-based screenings were carried out using these models against six distinct chemical databases (Chembridge Library, Maybridge Library, Asinex-Gold Library, Asinex-Platinum Library, SPECS database and NCI (National Cancer Institute) with the software Catalyst.^[30] The pharmacophore model in Figure 1 which gave the highest number of hits upon screening, was chosen to be the starting point. The hit compounds with a fit value higher than 2.5 (number of matching pharmacophore points, the maximum being five) were selected for further evaluation for Lipinski's rule of five with MOE.^[32] The compounds that satisfy Lipinski's rule of five were subjected to the docking process with AutoDock 4.0, AutoDock Vina and Gold v5.1.

Furthermore, the pharmacophore model above was tested for its ability to discriminate active and inactive inhibitors. A small database composed of 66 active and 108 inactive compounds was created using the ChEMBL database^[31] of bioactive drug-like small molecules. The screening of the database using the selected pharmacophore model via LigandScout generated a ROC curve which lies well above the diagonal line of random hits, indicating that the model is able to select active inhibitors over inactive ones.

2.2 Docking

The crystal structure of PDEIV (PDB Code:1RO6) taken from the PDB databank was chosen because of its highest resolution and relatively intact structure.^[33] The target protein is a homodimer. At the binding site, the water molecule

which is found near the ligand and the two metal ions Zn^{+2} and Mg^{+2} , were kept fixed during the docking process. Using MOE, the polar hydrogens were added to the protein based on the protonation states of the ionizable side chains. Using AutoDockTools (or ADT, the GUI of AutoDock), Gasteiger charges were assigned to both the ligand and the macromolecule and non-polar hydrogens were merged to the bonded heavy atom based on the united atom model. For AutoDock 4.0, the docking process for screening was composed of 10 independent runs which yielded 10 docked conformations for each compound in the library. For conformational search, the simulated annealing methodology^[34] was used with its default parameters. A total of 150 distinct ligand conformers are initially generated and positioned randomly in the binding pocket. The number of energy evaluations are adjusted with respect to the number of torsions in the ligand based on the general guidelines of AutoDock. The target protein was held rigid during docking. A pre-calculated three-dimensional energy grid of equally spaced discrete points is generated prior to docking, for a rapid energy evaluation, using the program AutoGrid.^[35] The grid box with dimensions of $32 \text{ \AA} \times 72 \text{ \AA} \times 31 \text{ \AA}$ covers the entire binding site and its neighboring residues. The distance between two grid points is set to 0.375 \AA . AutoDock Vina uses the same molecular structure file format used by AutoDock 4.0. A precalculated three-dimensional energy grid map and assigning atom charges are not needed for Vina. The two major distinctions between two docking tools are the scoring function and the search algorithm.

The docking process was repeated with another docking tool, Gold v5.1. In Gold, a genetic algorithm (GA) was used to explore the full range of ligand conformational flexibility and the rotational flexibility of receptor hydrogens.^[26] The mechanism for ligand placement is based on fitting points. Among the four scoring functions provided in Gold (ChemPLP, GoldScore, ChemScore and ASP), ChemPLP was chosen due to its higher performance in pose prediction and virtual screening reported in the last few years. For defining the binding site, a spherical region surrounding the ligand with a radius of 12 \AA was chosen. All other variables were held fixed at their default values. 50 GA runs were carried out for each ligand.

Following the docking process, a total of 234 compounds with all three scoring values higher than those of rolipram were determined from AutoDock 4.0, AutoDock Vina and Gold v5.1. For each one of the 234 hit compounds, using the bound conformation with the highest AutoDock score, the interacting residues were determined and 117 out of 234 compounds were found to interact with at least five of the seven key residues. Afterwards, all 117 compounds were rescored using the DSX v.088 scoring function. This yielded a total of 101 compounds with better score values than that of the ligand rolipram. As a final step, toxicity calculation was carried out on FAF-Drugs2 server. FAF-Drugs2 (Free ADMET Filtering-Drugs2) is the

first free web-based package (<http://bioserv.rpbs.univ-paris-diderot.fr/FAF-Drugs/>) capable of preparing compound libraries through physicochemical rules, functional groups and Pan Assay Interference Compounds (PAINS) detection.^[36] Finally, 32 compounds passed the filtering test for ADME and toxicity (Table S1).

3 Results

3.1 Pharmacophore Models

Figures 1–4 show the pharmacophore points determined by LigandScout for four different crystal structures. In each figure, based on the residues surrounding the ligand and the excluded volume, potential interaction points on the ligand are highlighted as follows: a hydrophobic feature colored as a yellow sphere is the most common feature of all four models. Two other features are represented with red and green arrows representing the hydrogen bond acceptor and donor groups, respectively. Finally, the gray sphere represents the excluded volume. Two metal ions are represented with two small yellow spheres situated at the lower part of the figures.

In the 1RO6 complex crystal structure (see Figure 1), the co-crystallized ligand is rolipram. The aromatic ring and the five-membered ring at the top portion of the molecule represent the two hydrophobic features. In addition, the two red arrows represent the interactions between two oxygen atoms and Gln 443. At the lower portion, the carbonyl oxygen of heterocyclic ring interacts with the water molecule positioned between two metal ions, Zn⁺² and Mg⁺².

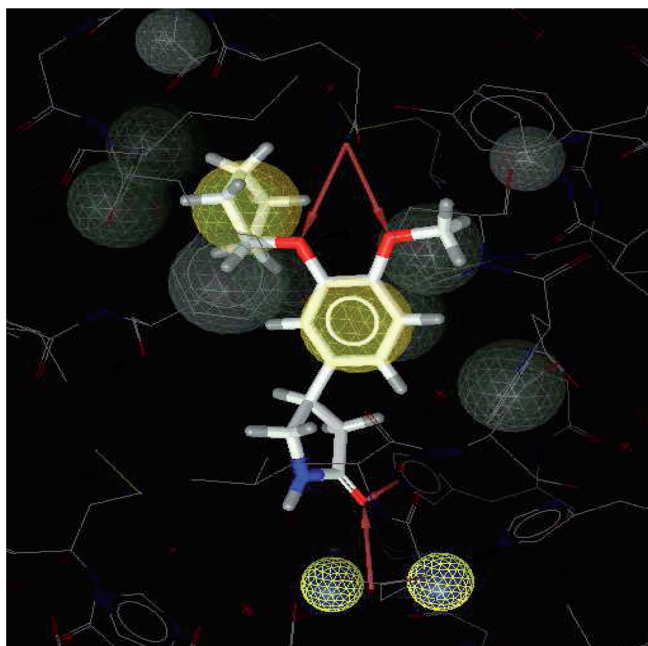


Figure 1. 1RO6 pharmacophore model.

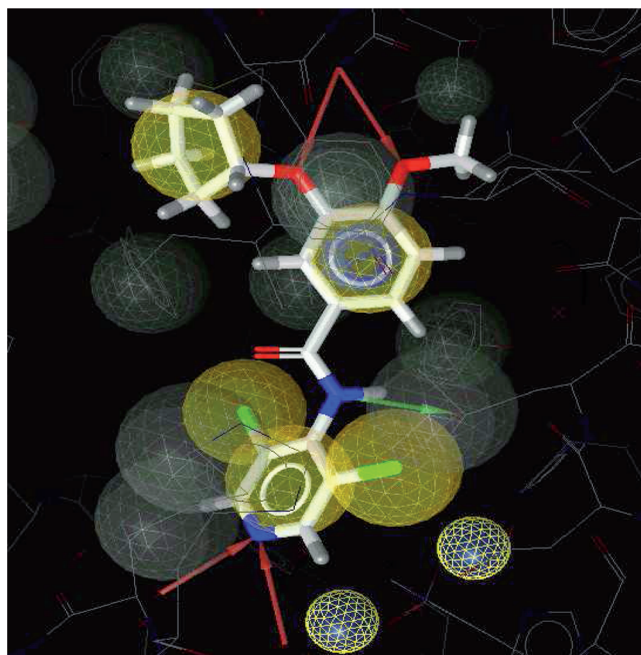


Figure 2. 1XM4 pharmacophore model.

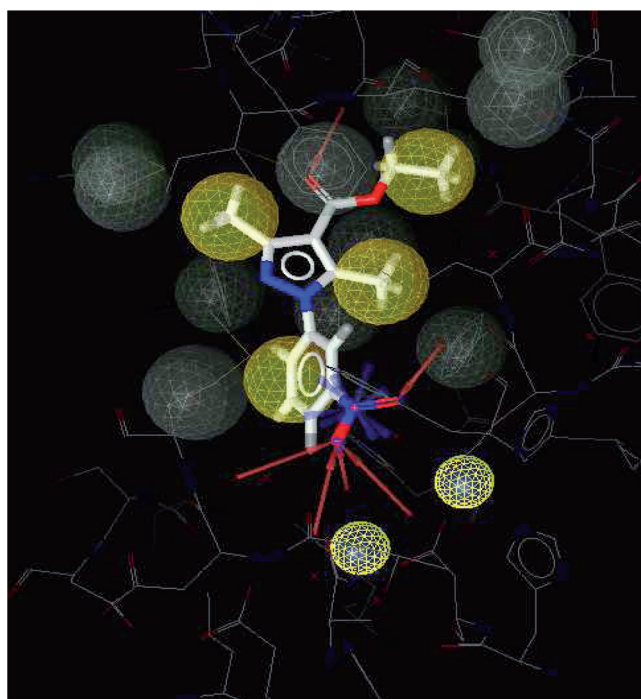


Figure 3. 1Y2J pharmacophore model.

In the 1XM4 complex crystal structure (see Figure 2), the ligand is piclomilast. As in 1RO6 complex, the two hydrophobic features and the hydrogen bond between two oxygen atoms and Gln 443 are present. In 1Y2J, 3,5-dimethyl-1-(3-nitro-phenyl)-1H-pyrazole-4-carboxylic acid ethyl ester is the ligand (Figure 3). The hydrophobic aromatic feature is the same as in the other two models, one of them

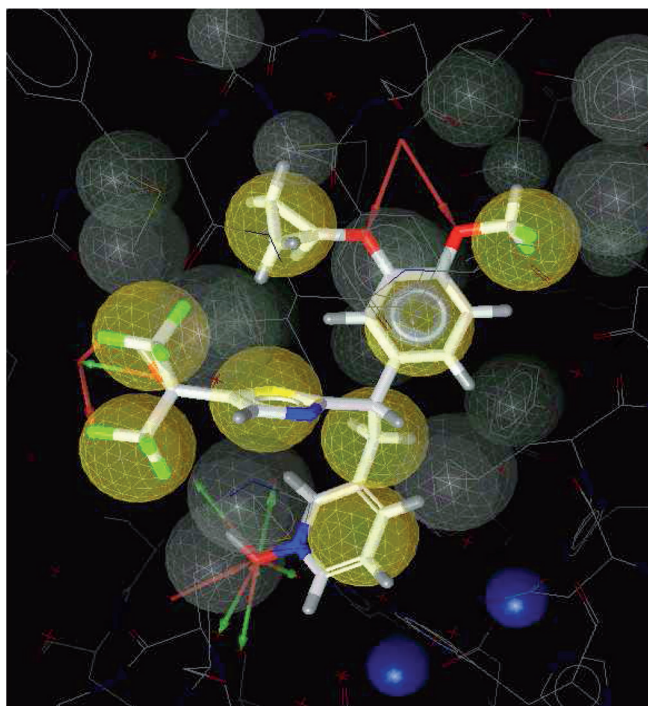


Figure 4. 2FM0 pharmacophore model.

being on the aromatic ring and the others on the methyl group attached to the five-membered ring. Also, as in 1RO6 model, the water molecule positioned between two metal ions, Zn^{+2} and Mg^{+2} , interacts with the oxygen at the lower portion of the molecule. In the last model, 2FM0 (see Figure 4), the ligand is (*S*)-3-(2-(3-cyclopropoxy-4-(difluoromethoxy)phenyl)-2-(5-(1,1,1,3,3,3-hexafluoro-2-hydroxypropan-2-yl)thiazol-2-yl)ethyl)pyridine 1-oxide (L-269298). As in 1RO6 complex, the two hydrophobic features and the hydrogen bond between two oxygen atoms and Gln 443 are present. The protein-ligand interactions for 1RO6 are displayed in Figure 5.

In order to display the common pharmacophore features of these four complex models, their ligands were structurally aligned with MOE as shown in Figure 6.

We have also examined six different crystal structures (PDEIV) which have the co-crystallized ligand rolipram: two are with the PDEIV B isoform (PDB codes: 1XN0 and 1XMY) and four are with the PDEIV D isoform (PDB codes: 1TBB, 1Q9M, 1OYN, and 3G4K). These six structures and the 1RO6 complex were aligned and superimposed with respect to the backbone (the root-mean-square deviation (rmsd) of each structure with respect to 1RO6 is found to be less than 1.7 Å) (Figure 7). The ligand rolipram from the crystal structure 1RO6 is shown in purple. Only in 1RO6, the five-membered ring in the ligand rolipram, is able to interact with the water molecule (HOH_788) and the two divalent metal ions (Zn^{+2} and Mg^{+2}). Because of its highest resolution and intact structure in the B isoform, the docking process was carried out with 1RO6.

3.2 Validation of the Pharmacophore Model

To further evaluate the selected pharmacophore model, a small database has been created using the ChEMBL database^[31] with a total of 2419 PDE4B inhibitors with known activity data. A total of 66 active and 108 inactive molecules has been selected using the information of K_i and inhibition percentage values: the compounds that have a K_i value smaller than $0.024 \mu\text{M}$ and/or an inhibition % value higher than 50 were selected as active inhibitors, whereas the compounds that have a K_i value greater than $223 \mu\text{M}$ and an inhibition % value smaller than 5 were selected as inactive (decoys) compounds. Compared to the K_i value of $0.221 \mu\text{M}$ ^[37] of the known inhibitor, rolipram, the highest K_i value of actives is 10 times lower, whereas the lowest K_i value of decoys is 1000 times higher than that of rolipram.

The pharmacophore screening of the small database via LigandScout has yielded 131 hits. The pharmacophore model consisted of a total of 14 pharmacophore features of which nine were excluded volume features (see Figure 1). For a molecule to be a hit, a minimum of nine features was necessary to exist. For different pharmacophore score values, the number of true positives (Se, % of selected active compounds) and false positives (1–Sp, % of decoys detected) have been determined and a ROC curve was obtained as shown in Figure 8. The area under the curve (AUC) has been determined as 1.0, 1.0, 1.0 and 0.76 in the top 1, 5, 10 and 100% of the screened database, respectively. In addition, the enrichment factor (EF) has been determined as 2.6, 2.6, 1.9, and 1.3 for 1, 5, 10 and 100% of the screened database, respectively (Figure 8). Overall, the validation study has shown that the selected pharmacophore model has a certain discriminatory power among the PDE4B active and decoy ligands in the ChEMBL database.

3.3 Virtual Screening via Docking

As our reference molecule, rolipram was first docked to the active site of the enzyme. The results are sorted based on the binding energy, which is the score value of AutoDock (Table 1). The conformation with the lowest binding energy (or the highest score value) has an rmsd value of 0.81 \AA with respect to the known conformation in the crystal structure. Also, 8 out of 10 predicted poses have an rmsd value under 1 \AA , with binding energies between -8.17 and -8.00 kcal/mol . Only one out of 10 poses has failed to predict the native state and it has the lowest score value (or highest energy) and the highest rmsd value. The strong correlation between the score value and the rmsd value proves AutoDock 4.0 to be a satisfactory tool for molecular recognition studies of the PDEIV enzyme.

The docking process was also carried out for the potent inhibitors displayed in Scheme 1. Seven of these potent inhibitors are the co-crystallized ligands for different PDEIV complex structures extracted from the Protein Databank. Five of them correspond to PDEIV B isoform (PDB codes:

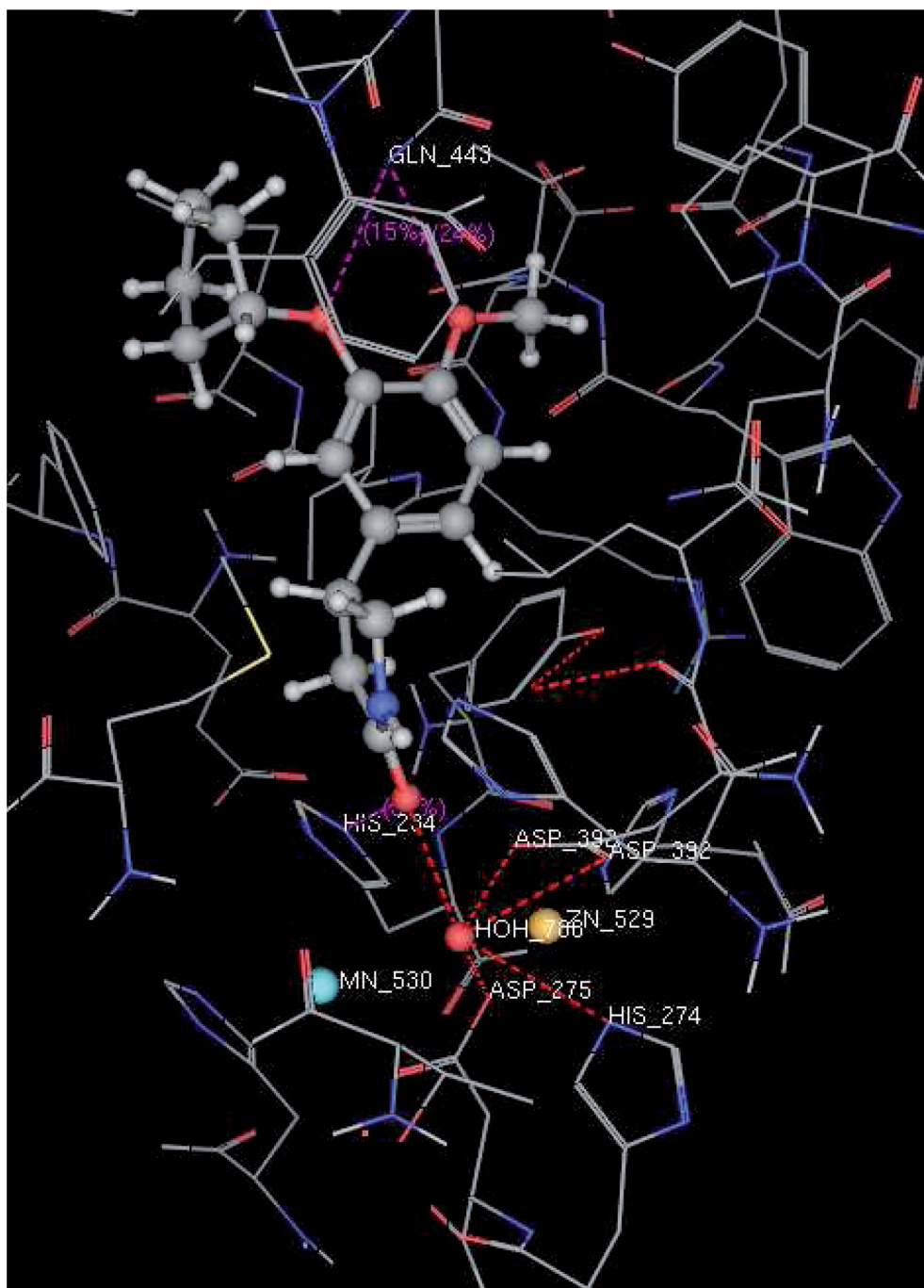


Figure 5. Protein–ligand interactions for 1RO6 with ligand rolipram.

1XM4 with piclamilast, 1XLZ with filaminast, 1XLX with cilomilast, 1XM6 with mesopram and 1XMU with roflumilast) and two of them belong to PDEIV D isoform (PDB codes: 1 MKD with zardaverine and 1ZKN with IBMX). These potent inhibitors were individually docked into their complex crystals with AutoDock 4.0, AutoDock Vina and Gold v5.1. Furthermore, they were also docked into the 1RO6 active site. In Table 2, the second column represents the

binding energy values with AutoDock when the ligands were docked into the 1RO6 active site and the last column shows the corresponding values when the ligands were docked into their own co-crystallized structures. As seen in Figure 9, AutoDock (1RO6), AutoDock (co-crystallized) and AutoDock Vina yield the same trend in binding energies; e.g. cilomilast and IBMX have the highest and lowest binding energies respectively. Interestingly, a similar trend was

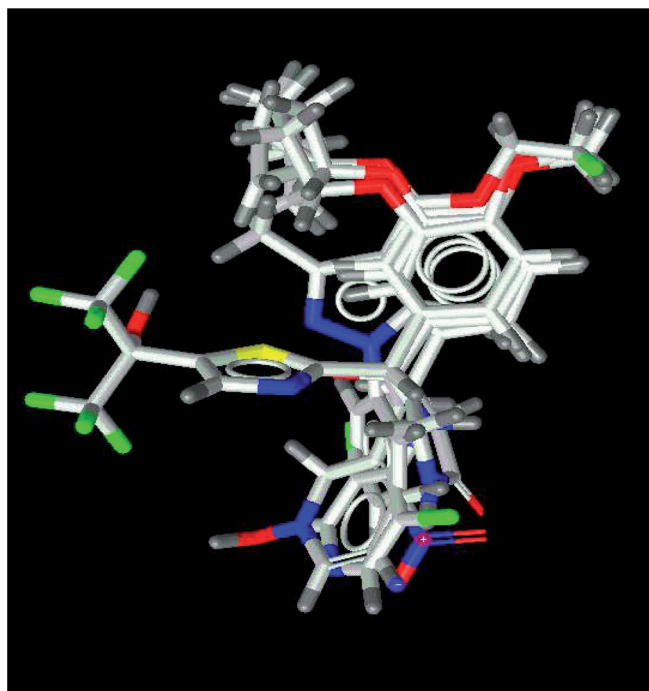


Figure 6. Ligand alignment with MOE.

also seen with Gold CHEMPLP score values demonstrating the high correspondence between the docking methodologies used in this study.

Following rolipram, 1840 candidate molecules that satisfy the criteria described in Methodology, were put to a virtual screening via AutoDock v 4.0, using the same docking parameters used for rolipram. For each ligand, the lowest binding energy (highest score) value was extracted. A total of 635 molecules were found to have a binding energy lower than that of rolipram.

Similarly, all 1840 molecules were subjected to a docking process via AutoDock Vina. It was proposed that Vina significantly improves the average accuracy of the binding mode predictions compared to AutoDock v4.0, judging by the tests on the training set used in AutoDock v4.0 development. Similar to AutoDock v4.0, rolipram was first docked with Vina, to check the performance in prediction. Vina was several orders of magnitude faster than AutoDock

Table 1. Docking results for ligand rolipram with AutoDock 4.0.

Rank (sub-rank)	Run	Binding energy (kcal/mol)	Reference RMSD (Å)
1 (1)	2	-8.17	0.81
1 (2)	5	-8.16	0.79
1 (3)	10	-8.16	0.79
1 (4)	1	-8.16	0.78
1 (5)	9	-8.16	0.82
1 (6)	8	-8.16	0.80
1 (7)	4	-8.16	0.78
1 (8)	3	-8.00	0.86
1 (9)	6	-7.27	1.53
2 (1)	7	-6.13	18.85

v4.0 and the conformation with the lowest binding energy (or the highest score) had an rmsd value of 0.73 Å, which is slightly closer to the native state (0.81 Å in AutoDock v4.0). As a result of docking 1840 compounds with AutoDock Vina, 489 compounds that had better binding affinities than that of rolipram were found.

Finally, the docking process was carried out by using Gold v5.1 using the scoring function ChemPLP. 681 compounds that had better CHEMPLP score values than that of rolipram, were selected as a result of this docking process.

The next step consists of combining the results from AutoDock v4.0, AutoDockVina and Gold v5.1. A total of 234 compounds were found to have stronger binding energies (higher scores) than rolipram in all three docking experiments, thus were selected for further analysis.

3.4 Protein-Ligand Interaction Maps

In this part of the study, two-dimensional protein-ligand interaction maps for known potent inhibitors (Scheme 1) and for the 234 hit molecules were created with MOE. First, the ligand interaction maps for the known potent inhibitors were analyzed and five key amino acid residues (Asn 395, Gln 443, Tyr 233, Ile 410, Phe 446) were observed to interact with more than 90% of the 14 known potent inhibitors (Figure 10). In addition to five key residues, in almost all potent molecules, Asp 275 and Asp 392 were observed in

Table 2. Docking results of potent ligands with AutoDock 4.0, AutoDock Vina and Gold v5.1.

Potent inhibitors	Binding energy AutoDock 4.0 [a]	Binding affinity AutoDock Vina [a]	Gold CHEMPLP Score [a]	Binding energy AutoDock 4.0 [b]
1.Zardaverine (1 MKD)	-6.56	-8.2	64.7323	-6.31
2.Roflumilast(1XMU)	-6.98	-9.2	70.6268	-6.90
3.Piclamilast(1XM4)	-8.03	-8.9	73.1025	-7.90
4.Mesopram(1XM6)	-6.62	-8.1	62.8033	-7.39
5.IBMX(1ZKN)	-5.83	-6.7	55.278	-5.96
6.Filaminast(1XLZ)	-6.96	-7.5	76.1991	-7.64
7.Cilomilast(1XLX)	-12.93	-9.7	92.3694	-11.02

[a] Target is the PDEIV in 1RO6. [b] Target is the PDEIV in their own co-crystallized complexes.

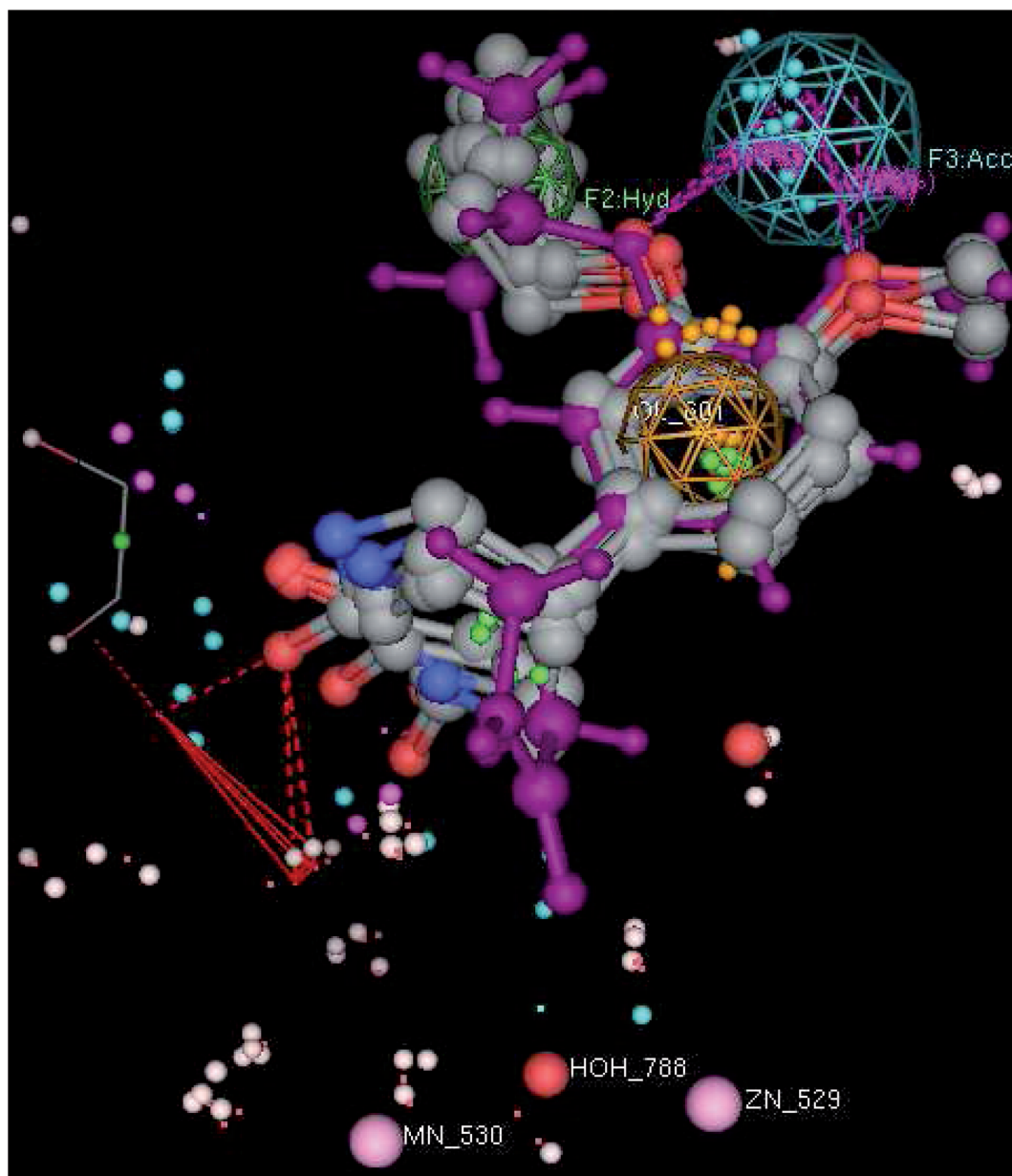


Figure 7. The alignment of seven crystal structures co-crystallized with rolipram.

the active site to coordinate with Mg^{+2} , Zn^{+2} and water, as seen in Figure 11.

For the 234 hit molecules, similar protein-ligand interaction maps were prepared and the percentage of occurrences of residues in the active site of the enzyme were calculated (Figure 12). As seen in Figure 12, a total of five residues interact with more than 80% of the hit compounds and they are Asp 392, His 234, Tyr 233, Ile 410, and Phe 446. Three of these five residues which are Tyr 233, Ile 410, and Phe 446 also interact with more than 90% of the known potent inhibitors as shown in Figure 10.

Furthermore, two residues which are Asp 392 and Thr 407 are observed to interact with more than 80%, but less

than 90% of the known potent inhibitors. Hence, they are selected as key residues in the binding site in addition to five key residues for the potent inhibitors mentioned above. Consequently, a total of seven selected key residues were inspected in the interaction maps of the hit molecules for which the bound conformation with the highest AutoDock score was used. Among the 234 hit compounds, 117 molecules were found to interact with at least five of the seven key residues and thus were selected for the next round of analysis where they were subjected to a knowledge-based scoring function called DSX.

For each of the 117 compounds, the conformation with the highest score obtained previously from AutoDock v4.0

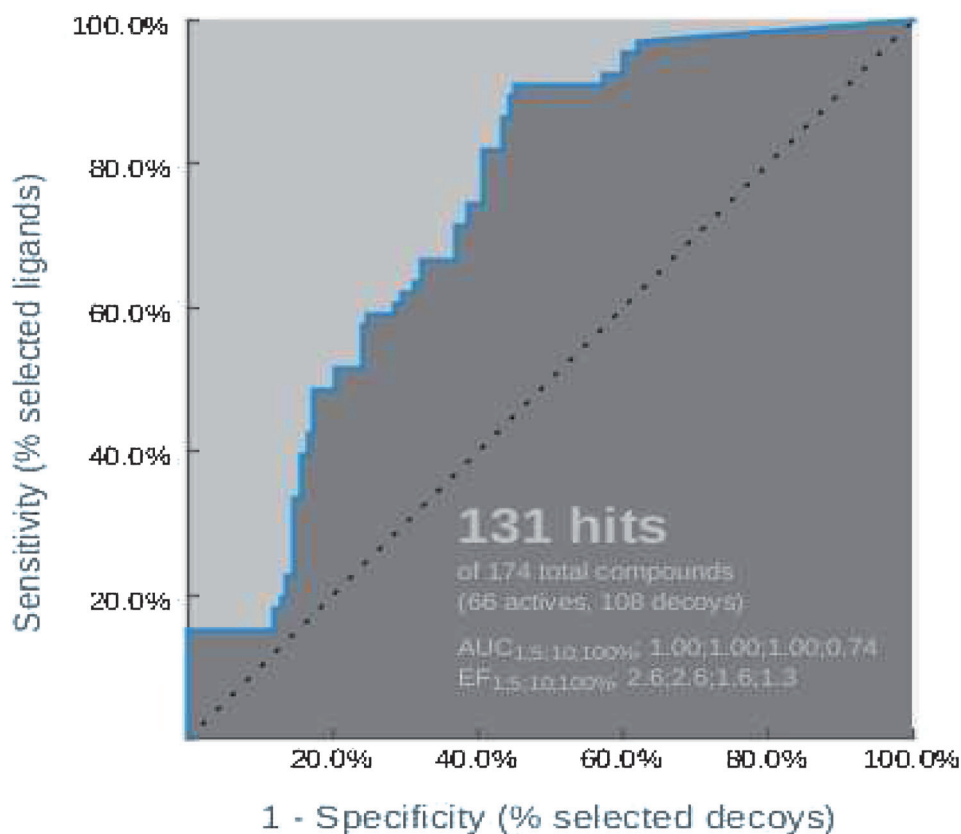


Figure 8. ROC curve obtained for the selected pharmacophore model. AUC and EF values are also provided for 1, 5, 10 and 100% of the selected database.

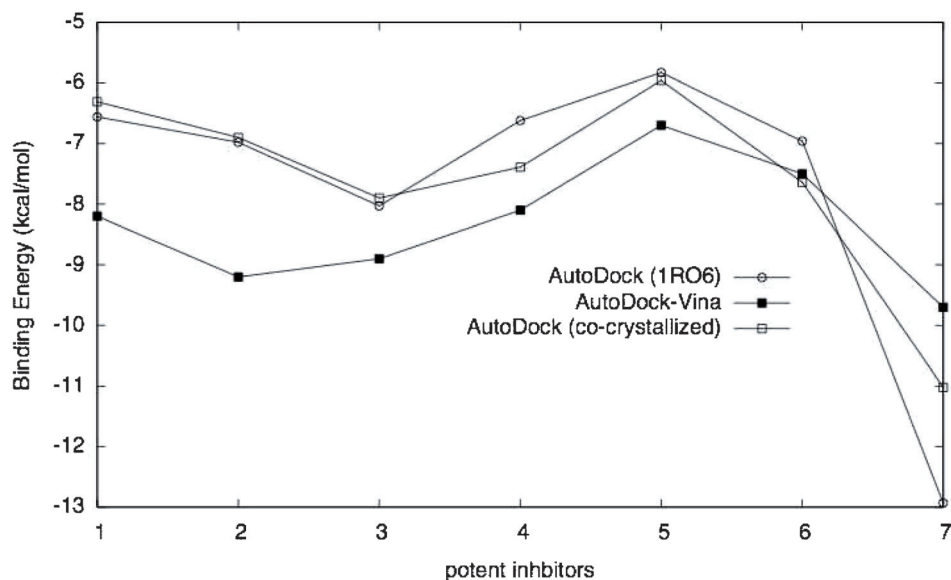


Figure 9. The correlation between the AutoDock scores docked into 1RO6 and the co-crystallized complexes.

was selected and its score value was determined using DSX. Rolipram's known conformation in the crystal structure was also rescored with DSX and taken as the lower

limit. A total of 101 compounds that had higher DSX score values than the lower limit were selected for further tests. Analysis of the structure of the hit compounds shows that

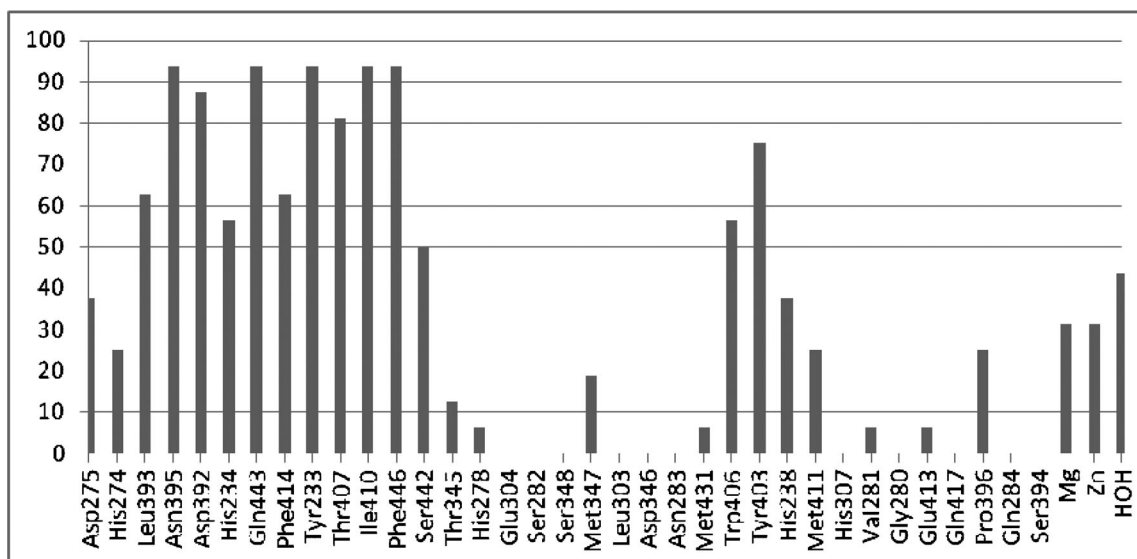
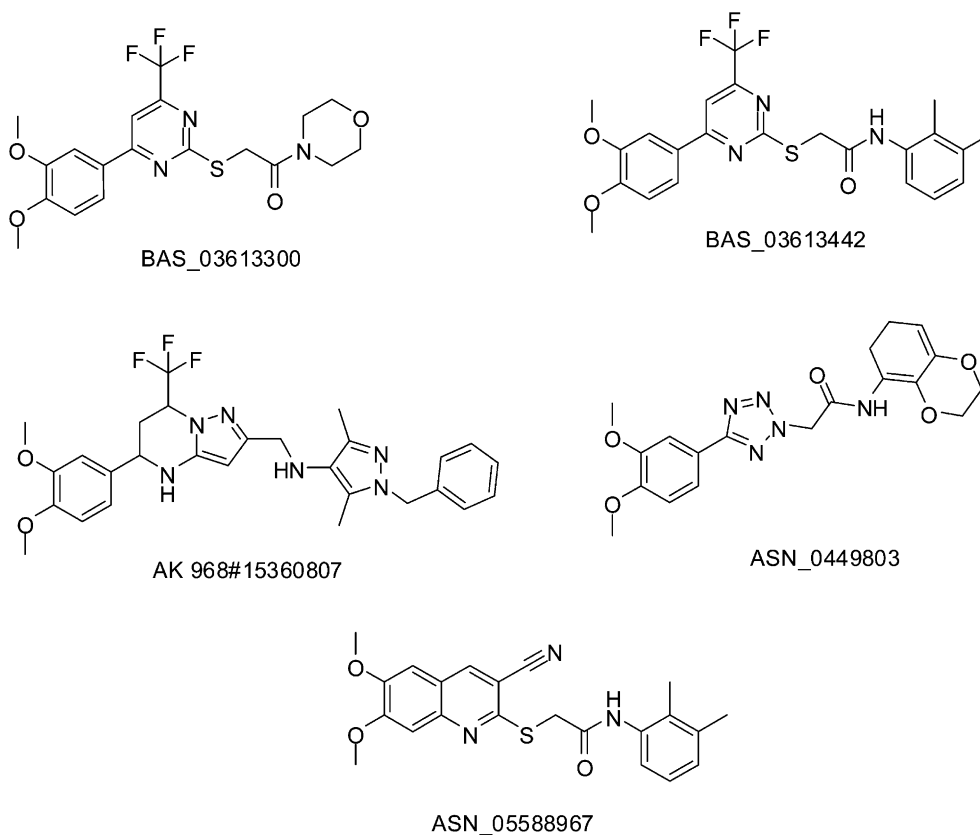


Figure 10. Percentage values of amino acid residues in the active site of the enzyme for known potent inhibitors.

the trifluoromethyl ($-\text{CF}_3$) and the 1,3-dimethoxybenzene ($-\text{C}_6\text{H}_4(\text{OCH}_3)_2$) groups are the common functional groups shared by most of the compounds. The trifluoromethyl group ($-\text{CF}_3$) interacts with two key residues Tyr 233, Asp 392 and the 1,3-dimethylbenzene interacts with another

key residue Gln 443 within a proximity of about 4 Å. These residues were previously shown to be present in both known potent inhibitors and hit compounds with high percentages.



Scheme 2. Candidate inhibitor molecules which have the highest pharmacophore fit values (greater than 3.8).

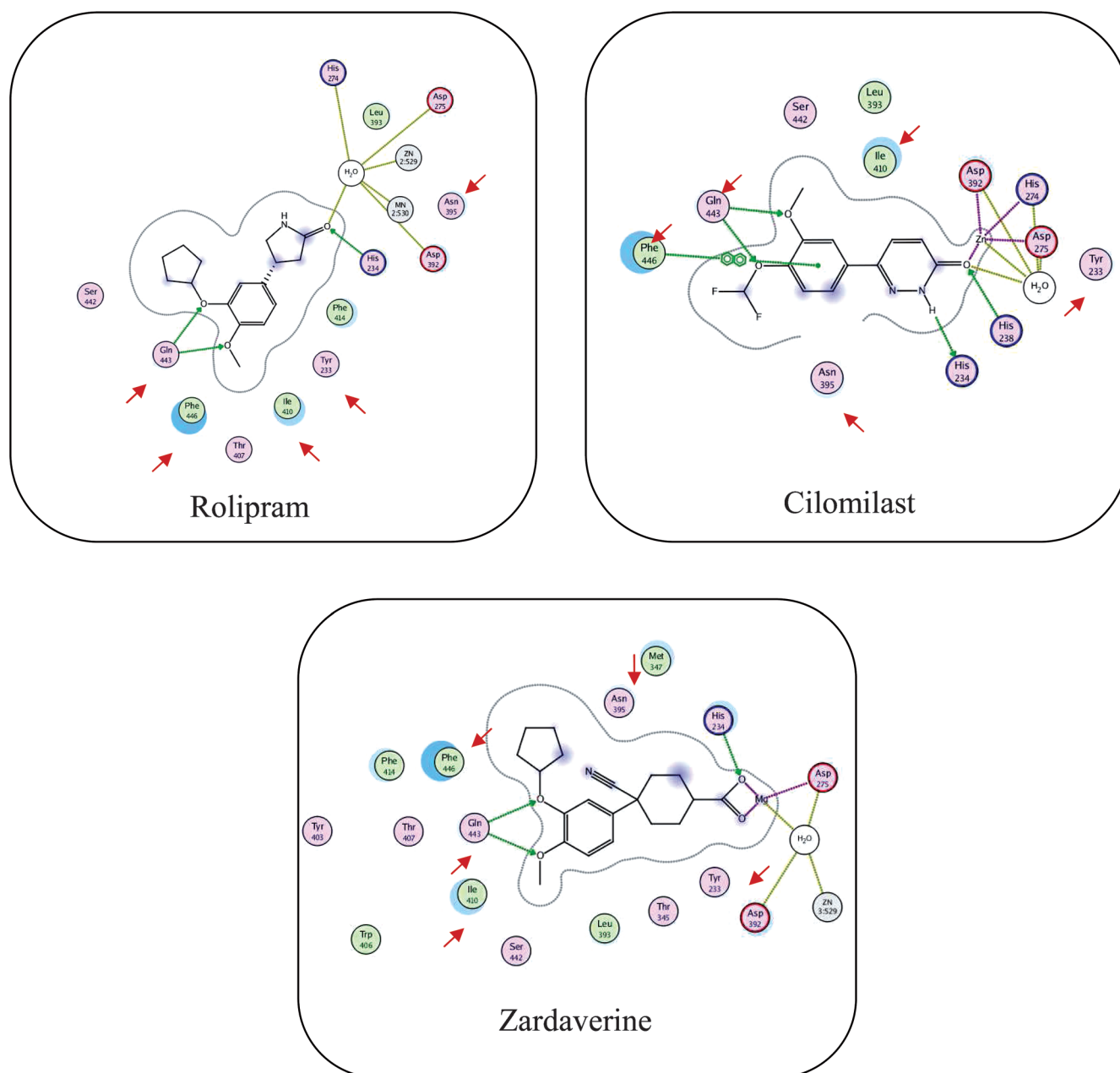


Figure 11. Ligand interaction maps for some potent inhibitors created with MOE.

As the final step of screening, 101 compounds were subjected to ADME/toxicity filtering on FAF-Drugs2 server and 32 of them which passed the test were proposed as candidates for the novel PDEIV inhibitors as shown in Scheme 2 (All the structures for the proposed novel inhibitors are displayed in the SI). Novel candidate inhibitors have a dimethoxyether aromatic ring as in rolipram. The flowchart that illustrates each step of the screening used in this study is displayed in Figure 13.

4 Conclusions

In this study, pharmacophore models were derived from four different protein-ligand crystal structures and they were employed to screen Cambridge Library, Maybridge Library, Asinex-Gold Library, Asinex-Platinum Library, SPECS database and NCI for the detection of PDEIV inhibitors. After the docking process with AutoDock v4.0, AutoDock Vina, and Gold v5.1, 234 inhibitors with score values higher than those of rolipram in all three docking experiments were determined as initial hit compounds. The ligand inter-

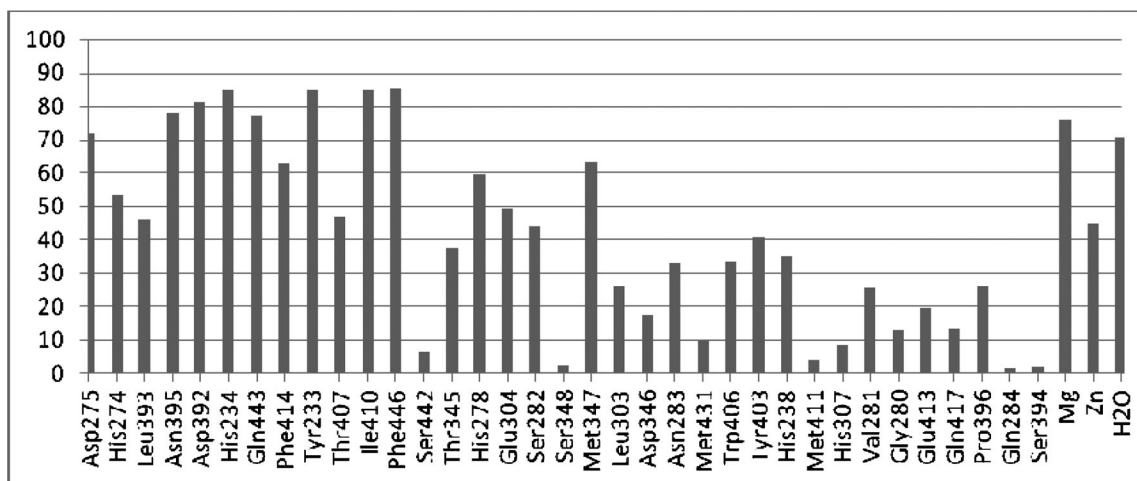


Figure 12. Percentage values of interactions observed in the active site of the enzyme with docked ligands.

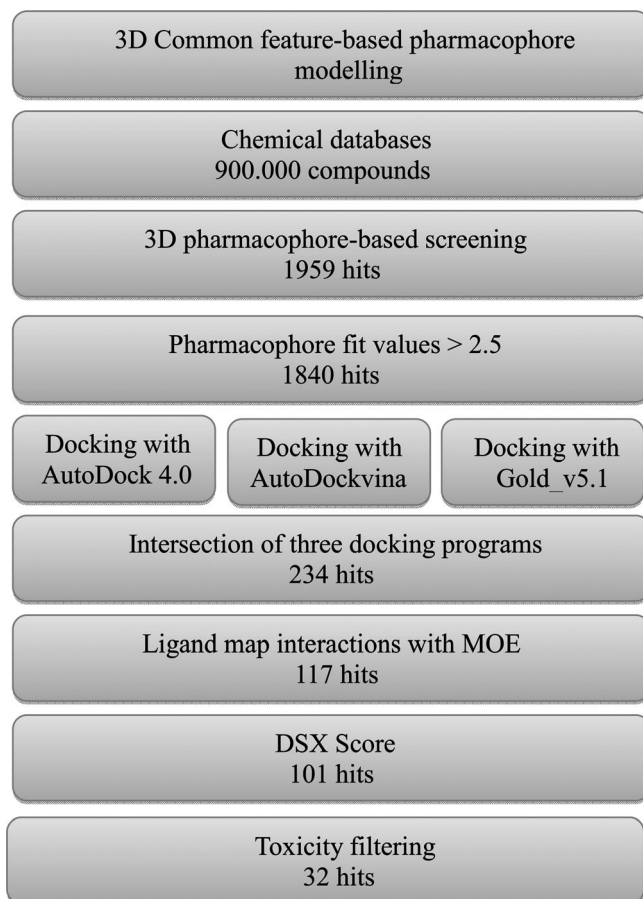


Figure 13. A flowchart depicting the procedure followed in this study.

action maps for the 14 known potent PDEIV inhibitors reveal seven key residues: Asn 395, Gln 443, Tyr 233, Ile 410, Phe 446, Asp 392 and Thr 407 which interact with

more than 80% of the potent inhibitors. The analysis of 2D protein-ligand interaction maps revealed that 117 out of 234 compounds interact with at least five of the seven key residues. Therefore, they were selected for further analysis which consists of rescoring with DSX scoring function. Rescoring yielded 101 compounds with DrugScore values less than -95.56 which belongs to rolipram. All 101 compounds were subjected to ADME/toxicity and only 32 of them which passed the filtering were proposed as the most promising compounds for novel PDEIV inhibitors. Molecules which have the highest pharmacophore fit values -greater than 3.8- were proposed as candidate inhibitors (see Scheme 2).

Acknowledgements

The authors gratefully acknowledge the guidance of Prof. G. Wolber and Dr. S. Distinto during the stay of G. Cifci in the Institute of Pharmacy, Department of Pharmaceutical Chemistry, Leopold-Franzens-University, Innsbruck, Austria. The authors thank the Boğaziçi Üniversitesi Bilimsel Araştırma Projeleri (09B502D) and TUBITAK (109T054) for computational power and financial support.

References

- [1] M. D. Houslay, G. Milligan, *Tr. Biochem. Sci.* **1997**, *22*(6), 217–224.
- [2] M. D. Houslay, M. Sullivan, G. B. Bolger, *Adv. Pharmacol.* **1998**, *44*, 225–342.
- [3] F. A. Antoni, *Front. Neuroendocrinol.* **2000**, *21*(2), 103–132.
- [4] T. J. Torphy, *Am. J. Respir. Crit. Care Med.* **1998**, *157*(2), 351–370.
- [5] M. Conti, S. L. C. Jin, *Prog. Nucleic Acid Res. Mol. Biol.* Vol 63 **2000**, *63*, 1–38.
- [6] S. H. Soderling, J. A. Beavo, *Curr. Opin. Cell Biol.* **2000**, *12*(2), 174–179.

- [7] J. D. Corbin, S. H. Francis, *J. Biol. Chem.* **1999**, *274*(20), 13729–13732.
- [8] V. C. Manganiello, M. Taira, E. Degerman, P. Belfrage, *Cell. Signal.* **1995**, *7*(5), 445–455.
- [9] C. Mehats, C. B. Andersen, M. Filopanti, S. L. C. Jin, M. Conti, *Tr. Endocrinol. Metabol.* **2002**, *13*(1), 29–35.
- [10] T. Muller, P. Engels, J. R. Fozard, *Tr. Pharmacol. Sci.* **1996**, *17*(8), 294–298.
- [11] W. J. Thompson, *Pharmacol. Ther.* **1991**, *51*(1), 13–33.
- [12] A. Castro, M. J. Jerez, C. Gil, A. Martinez, *Med. Res. Rev.* **2005**, *25*(2), 229–244.
- [13] K. H. Banner, M. A. Trevethick, *Trends Pharmacol. Sci.* **2004**, *25*(8), 430–436.
- [14] R. Draheim, U. Egerland, C. Rundfeldt, *J. Pharmacol. Exp. Ther.* **2004**, *308*(2), 555–563.
- [15] P. Jeffery, *Pulmon. Pharmacol. Ther.* **2005**, *18*(1), 9–17.
- [16] J. M. O'Donnell, H. T. Zhang, *Tr. Pharmacol. Sci.* **2004**, *25*(3), 158–163.
- [17] D. Spina, *Curr. Drug Targets Inflamm. Allergy* **2004**, *3*(3), 231–236.
- [18] Q. Huai, H. C. Wang, Y. J. Sun, H. Y. Kim, Y. D. Liu, H. M. Ke, *Structure* **2003**, *11*(7), 865–873.
- [19] Y. H. Jeon, Y. S. Heo, C. M. Kim, Y. L. Hyun, T. G. Lee, S. Ro, J. M. Cho, *Cell. Mol. Life Sci.* **2005**, *62*(11), 1198–1220.
- [20] K. F. Rabe, E. D. Bateman, D. O'Donnell, S. Witte, D. Bredenkroder, T. D. Bethke, *Lancet* **2005**, *366*(9485), 563–571.
- [21] P. M. A. Calverley, F. Sanchez-Torill, A. Mclvor, P. Teichmann, D. Bredenkroder, L. M. Fabbri, *Am. J. Respir. Crit. Care Med.* **2007**, *176*(2), 154–161.
- [22] A. P. Skoumbourdis, R. Huang, N. Southall, W. Leister, V. Guo, M. H. Cho, J. Inglese, M. Nirenberg, C. P. Austin, M. Xia, C. J. Thomas, *Bioorg. Med. Chem. Lett.* **2008**, *18*(4), 1297–1303.
- [23] M. D. Houslay, G. S. Baillie, D. H. Maurice, *Circ. Res.* **2007**, *100*(7), 950–966.
- [24] G. M. Morris, D. S. Goodsell, R. S. Halliday, R. Huey, W. E. Hart, R. K. Belew, A. J. Olson, *J. Comput. Chem.* **1998**, *19*(14), 1639–1662.
- [25] O. Trott, A. J. Olson, *J. Comput. Chem.* **2010**, *31*(2), 455–461.
- [26] G. Jones, P. Willett, R. C. Glen, A. R. Leach, R. Taylor, *J. Mol. Biol.* **1997**, *267*(3), 727–48.
- [27] H. Gohlke, M. Hendlich, G. Klebe, *J. Mol. Biol.* **2000**, *295*(2), 337–356.
- [28] D. Lagorce, O. Sperandio, H. Galons, M. A. Miteva, B. O. Villoutreix, *Bmc Bioinformatics* **2008**, *9*.
- [29] G. Wolber, T. Langer, *J. Chem. Inf. Model.* **2005**, *45*(1), 160–169.
- [30] J. Kirchmair, G. Wolber, C. Laggner, T. Langer, *J. Chem. Inf. Model.* **2006**, *46*(4), 1848–1861.
- [31] A. Gaulton, L. Bellis, J. Chambers, M. Davies, A. Hersey, Y. Light, S. McGlinchey, R. Akhtar, F. Atkinson, A. P. Bento, B. Al-Lazikani, D. Michalovich, J. P. Overington, *Nucleic Acids Res.* **2011**, *40*, 1100–1107.
- [32] I. Chemical Computing Group, Montreal, Quebec, Canada, Molecular, Operating Environment (MOE).
- [33] Z. Chen, G. Tian, Z. Wang, H. Jiang, J. Shen, W. Zhu, *J. Chem. Inf. Model.* **2010**, *50*(4), 615–625.
- [34] O. Dym, I. Xenarios, H. Ke, J. Colicelli, *Mol. Pharmacol.* **2002**, *61*(1), 20–25.
- [35] R. H. Garrett M. Morris, Arthur J. Olson, unpublished results, **2008**.
- [36] J. B. Baell, G. A. Holloway, *J. Med. Chem.* **2010**, *53*(7), 2719–2740.
- [37] National Center for Biotechnology Information. PubChem Bio-Assay Database; AID=159939, Source=Scripps Research Institute Molecular Screening Center, <http://pubchem.ncbi.nlm.nih.gov/assay/assay.cgi?aid=159939>

Received: October 18, 2011

Accepted: May 15, 2012

Published online: July 11, 2012